Bioorganic Chemistry 90 (2019) 103074

Contents lists available at ScienceDirect

Bioorganic Chemistry

journal homepage: www.elsevier.com/locate/bioorg

One-step synthesis of methylene-bridged bis-carbazole and evaluation of its antitumor activity and G-quadruplex DNA binding property

Gang Li[c], Haodong Tang[a], Chuanfeng Liu[a], Xiaoyu Liao[c], Sicong Li[a], Zhengning Shu[a], Hui Yu[b], Peng Yang[a,c,*]

[a] Wuya College of Innovation, Shenyang Pharmaceutical University, Shenyang 110016, China
[b] School of Textile Materials and Engineering, Wuyi University, Jiangmen 529020, China
[c] Key Laboratory of Structure-Based Drug Design and Discovery of Ministry of Education, Shenyang Pharmaceutical University, Shenyang 110016, China

ARTICLE INFO

Keywords:
Carbazole
Methylene-bridge
Oligomer
DNA
Ligand

ABSTRACT

Most reported carbazolyl G-quadruplex DNA (G4-DNA) ligands possess a rigid structure rather than a flexible one. The conformationally flexible ligands are paid much less attention. In this study, we report a novel class of non-rigid methylene-bridged biscarbazolyl ligand and their G4-DNA binding properties. Moreover, the antitumor activities of all these oligomers have been evaluated. The results show that this family of oligomers could be facilely synthesized via solely one step. Among them, compound **2**, the bis-carbazole derivative, displays the best antitumor activity and IC_{50} values against HT-29, HepG2, A375 and MCF-7 cells are 0.69, 5.09, 3.15 and 3.8 μ mol/L, respectively. Although conformationally flexible, **2** is still capable of binding to as well as stabilizing G4-DNA via π-π stacking interaction. Moreover, **2** selectively binds to G4-DNA over duplex DNA. The current study enriches the category of carbazolyl G4-DNA ligands and paves the way for the search of more efficient G4-DNA ligands and antitumor leads.

1. Introduction

Carbazole alkaloids, isolated from the leaves of edible plant of *Murraya koenigii*, represent novel classes of natural drugs capable of curing a variety of diseases such as rheumatism, traumatic injury and etc [1]. In recent years, there is increasing interests to construct carbazole-based antitumor drugs ever since their DNA binding and anti-transcriptional activities have been found [2]. Through proper modifications, carbazoles could be able to interact with different DNA secondary structures including duplex, triplex and G-quadruplex (G4-DNA). G4-DNA ligands receive particular attentions nowadays as it is believed to hold great potential for the treatment of cancers [3]. A few carbazole-based G4-DNA ligands have been reported so far, including 3,6-bis(4-vinylpyridium)carbazoles (BMVCs), 3,6-bistriazolylcarbazole (BTC) and 3,6-bis-benzimidazolycarbazoles [4–6]. These compounds exhibit great G4-DNA binding abilities, telomerase inhibitory activities as well as excellent antiproliferative activities. These popular carbazole-based ligands have something in common, which is, in brief, that they all possess rigid and V-shape geometry. It is generally thought that the above structural feature would benefit their efficient overlapping with the G-quartet planes via π-π stacking interactions. Conversely, conformationally flexible carbazolyl G4-DNA ligands have been rarely reported so far [7].

In 2014, we synthesized a methylene-bridged non-rigid biscarbazole and found that it bound to duplex DNA much stronger than its monomer due to synergistic effect [8]. Later on, we constructed methylene-bridged carbazolyl cyclotrimers and cyclotetramers and found their three-way junction DNA and A-tract DNA binding properties [9–11]. Although methylene-bridged oligocarbazoles do not possess rigid geometry, they do interact with particular DNA conformations due possibly to their target-dependent self-adaptive conformations. With this idea in mind and following our long-term interests in DNA-ligands [8–14], we recently synthesized a novel series of linear carbazolyl oligomers. And, we also evaluated their antitumor activities and DNA binding abilities. To our joy, we found that the dimer compound **2** of this family exhibited excellent antitumor activity and displayed G4-DNA selective binding nature. We herein report our recent findings.

2. Experimental

2.1. General techniques

Unless otherwise noted, materials were obtained from commercial suppliers and were used without further purification. Thin layer

* Corresponding author.
E-mail address: yangpeng@syphu.edu.cn (P. Yang).

https://doi.org/10.1016/j.bioorg.2019.103074
Received 1 March 2019; Received in revised form 5 June 2019; Accepted 17 June 2019
Available online 19 June 2019

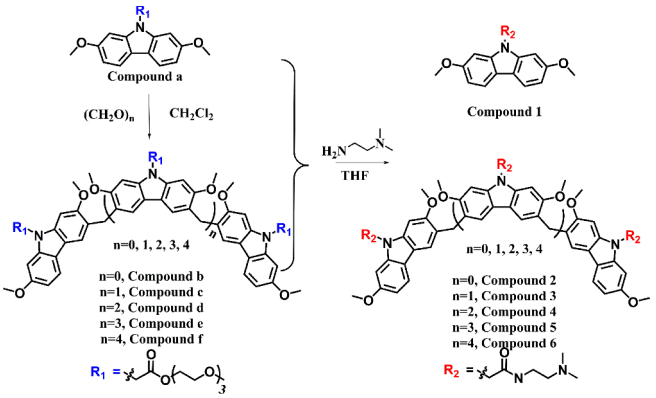

Scheme 1. the synthric routes for carbazolyl oligomers.

Table 1
IC_{50} values of all the tested compounds.

Compds.	IC_{50} (μ mol/L)			
	HT-29	HepG2	A375	MCF-7
1	40.57	59.56	40.57	63.23
2	**0.69**	**5.09**	**3.15**	**3.80**
3	59.54	69.37	5.43	85.68
4	34.98	44.09	36.74	57.94
5	22.33	51.39	43.07	58. 90
6	> 100	86.50	93.50	> 100
5-Fluorouracil	6.79	7.15	2.89	8.21
Doxorubicin	7.26	7.26	41.53	14.03
Paclitaxel	13.27	9.12	14.29	15.30

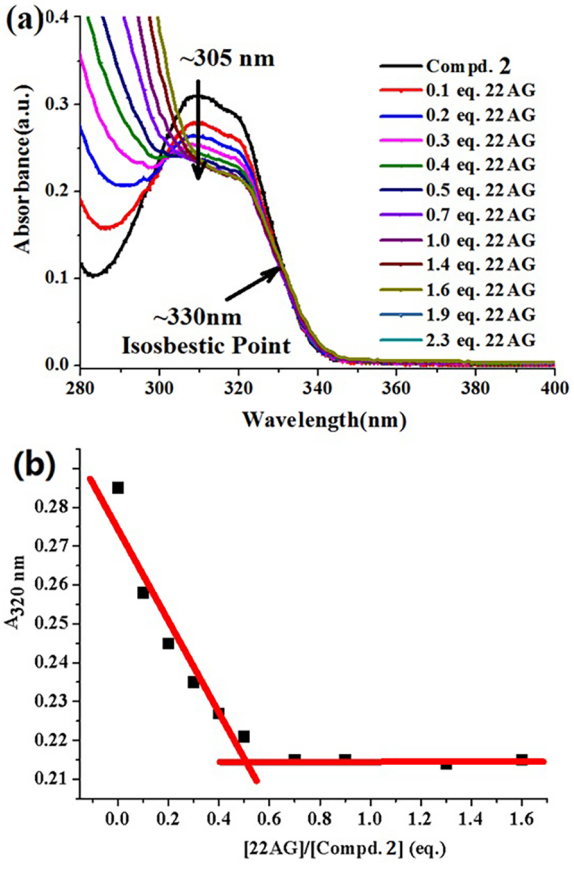

Fig. 1. (a) UV–vis spectra of 2 (15 μM) upon addition of 22AG. ; (b) The plotted curves of A_{320nm} of 2 as a function of 22AG concentration.

chromatography (TLC) analysis of reaction mixtures was performed on dynamic adsorbents silica gel F-254 TLC plates. Column chromatography was performed on silica gel 200–300 mesh. Fluorescence emission spectra were obtained using Shimadzu RF-5301 PC Spectrofluorophotometer. UV–vis absorption spectra were obtained on Beijing purkinje TU-1810. ^{1}H NMR (600 MHz) and ^{13}C NMR (150 MHz) spectra were recorded with Bruker Avance-III 600 spectrometers at 298 K. Chemical shifts were reported in units (ppm) and all coupling constants (*J* values) were reported in Hertz (Hz). High resolution mass spectra were obtained using Bruker micrOTOF-Q instrument with an ESI source.

For all the measurements, the solutions of compounds and DNA were freshly prepared before use. For UV–vis and fluorescence titrations, the stock solutions (20 mM, 200 mM and 500 mM, respectively) of target compounds were prepared by dissolving them in DMSO, the titrations were carried out in 10 mM PBS buffer (100 mM KCl, pH = 7.2, DMSO content: < 1.0%). For excitation and emission, the slit widths were 3 nm and 5 nm, respectively. For all measurements, excitation wavelength was 310 nm. Before the spectra were recorded, the sample solutions were mixed for 2 min after each addition of DNA.

2.2. G-quadruplex DNA preparation:

DNA were purchased from GenScrip®. The DNA strand were dissolved and mixed in PBS buffer (10 mM PBS buffer, 100 mM KCl, 1 mM EDTA, pH 7.2), heated to 95 °C for 5 min and slowly cooled down to room temperature to form the G-quadruplex. The volume of the solution was adjusted to a final concentration of 1.0 mM/duplex.

The DNA studied in this work were listed below:

DNA	Sequence
22AG	5′-AGGGTTAGGGTTAGGGTTAGGG-3′
ds16	5′-CACCGCTCTGGTCCTC-3′; 3′-GTGGACCAGAGCGGTG-5′

2.3. Synthesis method

Synthesis of TEG-derivated oligocarbazoles: A 1.0 g portion of compound **a** [10] and 188 mg of $FeCl_3$ were first mixed in 50 mL of CH_2Cl_2, and then 104 mg of polyformaldehyde was added to the solution. 2 h later, 50 mL solution of 3% NH_3 in water was added to the flask, extraction, the organic solvents were removed under vacuum. The residue was dried under reduced pressure and then purified by flash chromatography on silica gel using MeOH/CH_2Cl_2 (1:25, v/v) to give the desired products.

Compound b. Yield: 31%. ^{1}H NMR (600 MHz, $CDCl_3$), *δ* (ppm): 7.75 (m, 2H), 7.62 (s, 2H), 6.8 (s, 2H), 6.76–6.78 (m, 4H), 4.97 (s, 4H), 4.33 (t, *J* = 4.2 Hz, 4H), 4.20 (s, 2H), 3.94 (s, 6H), 3.89 (s, 6H), 3.67 (t, 4H), 3.57–3.59 (m, 4H), 3.50–3.54 (m, 12H), 3.36 (s, 6H). ^{13}C NMR (150 MHz, $CDCl_3$) *δ* 168.5, 158.0, 156.5, 141.5, 140.3, 122.6, 120.9, 120.1, 117.4, 116.2, 107.2, 93.2, 90.9, 71.8, 70.4, 70.4, 68.7, 64.7, 58.9, 55.8, 55.6, 44.7, 30.3.HRMS (ESI/TOF-Q) Calcd. for $[M+Na]^+$ 897.3780, found 897.3780.

Compound c. Yield: 26%. ^{1}H NMR (600 MHz, DMSO-d_6), *δ* 7.67 (d, *J* = 8.4 Hz, 2H), 7.49 (ss, 4H), 7.11 (ss, 4H), 6.99 (d, *J* = 1.8 Hz, 2H), 6.68 (d, J_1 = 8.4 Hz, J_2 = 1.8 Hz, 2H), 5.34 (s, 2H), 5.27 (s, 4H), 4.25 (t, *J* = 4.2 Hz, 2H), 4.21 (t, *J* = 4.2 Hz, 4H), 4.03 (s, 4H), 3.86 (s, 6H), 3.83 (s, 6H), 3.80 (s, 6H), 3.62 (t, *J* = 4.8 Hz, 2H), 3.60 (t, *J* = 4.8 Hz, 4H), 3.43–3.46 (m, 18H), 3.37–3.39 (m, 6H), 3.20 (s, 9H). ^{13}C NMR (150 MHz, DMSO-d_6) *δ* 169.4, 169.3, 157.9, 156.2, 156.1, 141.9, 140.7, 122.1, 121.6, 120.4, 120.2, 120.0, 116.7, 115.8, 115.6, 107.6, 99.0, 94.2, 92.5, 92.4, 71.6, 70.1, 70.1, 69.9, 68.6, 68.6, 64.6, 60.6, 58.4, 56.1, 56.0, 55.8, 30.3. HRMS (ESI/TOF-Q) Calcd. $[M+Na]^+$: 1340.5724, found: 1340.5679.

Compound d.Yield: 12%. ^{1}H NMR (600 MHz, DMSO-d_6), *δ* 7.66 (d,

J = 8.4 Hz, 2H), 7.47 (s, 2H), 7.44 (s, 2H), 7.41 (s, 2H), 7.09 (ss, 4H), 7.04 (s, 2H), 7.00 (s, 2H), 6.67 (d, J = 8.4 Hz, 2H), 5.29 (m, 8H), 4.22 (t, J = 4.2 Hz, 8H), 4.01 (s, 4H), 3.97 (s, 2H), 3.84 (s, 6H), 3.82 (s, 6H), 3.80 (s, 12H), 3.60 (t, J = 4.8 Hz, 8H), 3.40–3.45 (m, 24H), 3.35–3.38 (m, 8H), 3.20 (s, 6H), 3.18 (s, 6H). ^{13}C NMR (150 MHz, DMSO-d_6) δ 169.3, 169.3, 157.9, 156.2, 156.1, 156.0, 141.9, 140.6, 140.5, 140.4, 122.1, 121.8, 121.5, 120.4, 120.2, 120.1, 120.0, 116.7, 115.8, 115.7, 115.6, 107.7, 107.6, 94.2, 92.5, 92.4, 71.6, 71.6, 70.1, 70.1, 70.1, 70.0, 69.9, 69.9, 68.6, 64.6, 64.5, 58.4, 58.3, 56.1, 56.0, 56.0, 55.8, 44.4, 44.3. HRMS (ESI/TOF-Q) Calcd. $[M + 2Na]^{2+}/2$: 903.8803, found: 903.8940.

Compound e.Yield: 8%. ^{1}H NMR (600 MHz, DMSO-d_6), δ 7.66 (d, J = 8.4 Hz, 2H), 7.47 (ss, 4H), 7.41 (ss, 4H), 7.10 (ss, 4H), 7.04 (ss, 4H), 7.00 (s, 2H), 6.67 (d, J = 8.4 Hz, 2H), 5.27 (m, 10H), 4.20–4.23 (m, 10H), 4.02 (s, 4H), 3.97 (s, 4H), 3.86 (s, 6H), 3.83 (s, 6H), 3.79–3.80 (m, 18H), 3.58–3.60 (m, 10H), 3.37–3.46 (m, 40H), 3.20 (s, 6H), 3.19 (s, 6H), 3.17 (s, 3H). ^{13}C NMR (150 MHz, DMSO-d_6) δ 169.3, 169.3, 169.2, 157.9, 156.2, 156.2, 156.1, 156.0, 156.0, 141.9, 140.6, 140.5, 140.4, 140.4, 71.6, 71.6, 71.6, 70.1, 70.1, 70.1, 70.1, 70.0, 69.9, 69.9, 69.9, 68.6, 64.5, 58.4, 58.3, 58.3, 56.1, 56.0, 55.9, 55.8, 44.4, 44.3, 30.4. HRMS (ESI/TOF-Q) Calcd. $[M + 2Na]^{2+}/2$: 1125.4769, found: 1125.4763.

Compound f. Yield: 5%. ^{1}H NMR (600 MHz, DMSO-d_6), δ 7.64 (d, J = 8.4 Hz, 2H), 7.45 (ss, 4H), 7.37–7.39 (m, 6H), 7.09 (ss, 4H), 7.01–7.03 (m, 6H), 6.98 (s, 2H), 6.66 (d, J = 8.4 Hz, 2H), 5.24–5.28 (m, 12H), 4.19–4.21 (m, 12H), 4.01 (s, 4H), 3.96 (br, 6H), 3.84 (s, 6H), 3.82 (s, 6H), 3.77–3.79 (m, 24H), 3.56–3.59 (m, 12H), 3.36–3.45 (m, 48H), 3.19 (s, 6H), 3.17 (s, 6H), 3.15 (s, 6H). ^{13}C NMR (150 MHz, DMSO-d_6) δ 169.3, 169.3, 169.2, 157.9, 156.2, 156.1, 156.0, 141.9, 140.6, 140.5, 140.4, 121.8, 121.7, 120.2, 120.2, 120.2, 120.1, 120.1, 116.7, 115.8, 115.8, 115.7, 115.6, 107.6, 107.6, 107.5, 94.2, 94.2, 92.4, 92.3, 71.6, 71.6, 71.5, 70.1, 70.1, 70.1, 70.0, 69.9, 69.9, 69.8, 68.6, 64.5, 64.5, 64.5, 58.4, 58.3, 58.3, 56.1, 56.0, 55.9, 55.9, 55.7, 44.4, 44.3, 30.4. HRMS (ESI/TOF-Q) Calcd. $[M + 2Na]^{2+}/2$: 1347.0741, found: 1347.0788.

Synthesis of *N*, *N*′-dimethylethylenediamine-derivated oligocarbazoles: 25 mg of TEG-derivated compound **b (c, d, e, f)** and 1 mL of *N*, *N*′-dimethylethylenediamine were dissolved in 1 mL THF and then heated at 65 °C for 12 h. Afterwards, the cooled mixture was dropped into methanol to give the targets.

Compound 1: the syntheses of compound 1 followed our previously developed methods [10].

Compound 2: Yield 77%. ^{1}H NMR (600 MHz, DMSO-d_6) δ 8.15 (s, 2H), 7.71 (s, 2H), 7.56 (s, 2H), 7.11 (s, 2H), 7.00 (s, 2H), 6.69 (s, 2H), 4.95 (s, 4H), 4.08 (s, 2H), 3.89 (s, 6H), 3.81 (s, 6H), 3.20 (s, 4H), 2.30 (s, 4H), 2.13 (s, 12H). ^{13}C NMR (150 MHz, DMSO-d_6) δ 167.8, 157.9, 156.3, 142.1, 141.0, 121.7, 120.4, 120.0, 116.7, 115.7, 107.5, 94.2, 92.5, 58.5, 56.1, 55.8, 46.2, 45.5, 37.2, 30.4. HRMS (ESI/TOF-Q) Calcd. $[M + H]^+$: 723.3865; found: 723.3782.

Compound 3: Yield 71%. ^{1}H NMR (600 MHz, DMSO-d_6) δ 8.09 (br, 3H), 7.66 (d, J = 7.8 Hz, 2H), 7.48 (ss, J = 6.0 Hz, 4H), 7.08 (s, 2H), 6.97 (s, 2H), 6.66 (d, J = 7.8 Hz, 2H), 4.99 (s, 2H), 4.92 (s, 4H), 4.03 (s, 4H), 3.86 (s, 6H), 3.84 (s, 6H), 3.80 (s, 6H), 3.20 (br, 6H), 2.30 (br, 6H), 2.11 (br, 18H). ^{13}C NMR (150 MHz, DMSO-d_6) δ 167.9, 167.8, 157.9, 156.2, 156.1, 142.1, 140.8, 140.7, 122.0, 121.4, 120.5, 120.1, 120.0, 116.7, 115.8, 115.6, 107.4, 94.2, 92.5, 92.4, 58.5, 58.5, 56.0, 56.0, 55.7, 46.4, 46.2, 45.5, 45.5, 37.2, 37.1, 30.3. HRMS (ESI/TOF-Q) Calcd. $[M + 2H]^{2+}/2$: 545.7922; found: 545.7996.

Compound 4: Yield 63%. ^{1}H NMR (600 MHz, DMSO-d_6) δ 8.10 (br, 2H), 8.04 (br, 2H), 7.65 (d, J = 8.4 Hz, 2H), 7.41–7.45 (m, 6H), 6.97–7.05 (m, 8H), 6.65 (d, J = 7.2 Hz, 2H), 4.94 (s, 4H), 4.92 (s, 4H), 3.98–4.01 (m, 6H), 3.80–3.84 (m, 24H), 3.17 (br, 8H), 2.28 (br, 8H), 2.07–2.10 (m, 24H). ^{13}C NMR (150 MHz, DMSO-d_6) δ 167.9, 167.8, 157.9, 156.1, 156.1, 156.0, 142.1, 140.8, 140.7, 140.6, 122.0, 121.7, 121.3, 120.4, 120.2, 120.0, 120.0, 116.7, 115.8, 115.7, 115.6, 107.4, 94.2, 92.5, 92.4, 92.3, 58.5, 56.0, 56.0, 56.0, 46.3, 46.2, 45.5, 45.5, 37.1, 30.4. HRMS (ESI/TOF-Q) Calcd. $[M + H]^+$: 1457.7656; found: 1457.7642.

Compound 5: Yield 62%. ^{1}H NMR (600 MHz, DMSO-d_6) δ 8.15 (br, 2H), 8.10 (br, 2H), 8.05 (br, 1H), 7.64 (d, J = 8.4 Hz, 2H), 7.38–7.45 (m, 8H), 6.97–7.06 (m, 10H), 6.65 (d, J = 7.2 Hz, 2H), 4.92–4.96 (m, 10H), 3.97–4.01 (m, 8H), 3.79–3.84 (m, 30H), 3.17–3.20 (m, 10H), 2.32–2.37 (m, 10H), 2.11–2.17 (m, 30H). ^{13}C NMR (150 MHz, DMSO-d_6) δ 168.0, 167.9, 157.9, 156.2, 156.1, 156.0, 142.1, 140.8, 140.7, 140.6, 140.6, 122.0, 121.7, 121.6, 121.3, 120.5, 120.2, 120.0, 119.9, 116.7, 115.8, 115.7, 115.6, 107.4, 94.2, 92.5, 92.4, 58.2, 56.0, 56.0, 55.9, 55.7, 46.3, 46.1, 45.2, 45.1, 36.8, 36.7, 30.4. HRMS (ESI/TOF-Q) Calcd. $[M + 2H]^{2+}/2$: 913.4835; found: 913.4813.

Compound 6: Yield 72%. ^{1}H NMR (600 MHz, DMSO-d_6) δ 8.09 (br, 2H), 8.03 (br, 2H), 7.98 (br, 2H), 7.62 (d, J = 7.8 Hz, 2H), 7.36–7.44 (m, 10H), 6.96–7.05 (m, 12H), 6.64 (d, J = 7.2 Hz, 2H), 4.90–4.96 (m, 12H), 3.95–4.00 (m, 10H), 3.77–3.84 (m, 36H), 3.13–3.17 (m, 12H), 2.21–2.28 (m, 12H), 2.03–2.09 (m, 36H). ^{13}C NMR (150 MHz, DMSO-d_6) δ 167.8, 167.8, 167.7, 157.8, 156.1, 156.1, 156.0, 142.1, 140.8, 140.7, 140.6, 140.6, 140.5, 122.0, 121.7, 121.6, 121.6, 121.3, 120.3, 120.2, 120.2, 120.1, 120.1, 120.0, 116.7, 115.8, 115.8, 115.7, 115.7, 115.5, 94.2, 92.5, 92.3, 58.5, 58.4, 56.0, 56.0, 55.9, 55.9, 55.7, 46.3, 46.1, 45.5, 45.4, 37.1, 37.1, 30.4. HRMS (ESI/TOF-Q) Calcd. $[M + 4H]^{4+}/4$: 548.7922 found: 548.7944.

2.4. UV-melting

The profiles of UV absorbance versus temperature were measured by monitoring absorption at 260 nm (ds16) and 295 nm (22AG), respectively. The concentration of DNA in each sample was 5 μM in 10 mM PBS buffer (pH 7.2). The experiments were carried out by increasing the temperature from 15 °C to 85 °C.

2.5. Cytotoxicity assay

Cells were seeded into 96-well cell culture plates (Corning, NY, USA) at a density of 5×10^3 cells per well and cultured for 24 h. Next, cells were subsequently incubated in presence of increasing concentrations (0 to 100 μM) of ligands at 37 °C for 48 h. After treatment, the cells were rinsed twice with ice-cold PBS and incubated with 100 μL of 0.5 mg/mL MTT (3-(4,5-dimethylthiazolyl-2)-2,5-diphenyl-tetrazolium bromide, Sigma-Aldrich) solution at 37 °C for 3 h. The supernatant were discarded and the residual cell layer was dissolved in 150 μL of DMSO, and optical density was measured using a microplate reader (Thermo Scientific, Shanghai, China). Cell viability was calculated using the following equation:

$$\text{Cell growth inhibitory ratio (\%)} = 100 \times (A_{530,\text{control}} - A_{530,\text{sample}})/(A_{530,\text{control}} - A_{530,\text{blank}})$$

3. Results and discussion

3.1. Synthesis

Up to now, only few methodologies have been proposed for the preparation of methylene bridges of carbazoles and one-step stratergy is even rarer [15,16]. As mentioned earlier, in 2014, we developed a method of preparing the methylene bridged bis-carbazole *via* an ipso-substitution (or ipso-alkylation) process. In that strategy, however, the aldehyde group should be constructed in advance and the total yield for the biscarabzole was only ~10%.

In 2016, we developed a one-step Lewis-acid catalyzed strategy to prepare carbazolyl cyclomers in diluted CH_2Cl_2 solution [9]. We now proposed a method to synthesize linear oligomeric carbazoles: the reaction was carried out by using a concentrated solution of the reactant in CH_2Cl_2 and using $FeCl_3$ as the catalyst. In this way, a series of linear

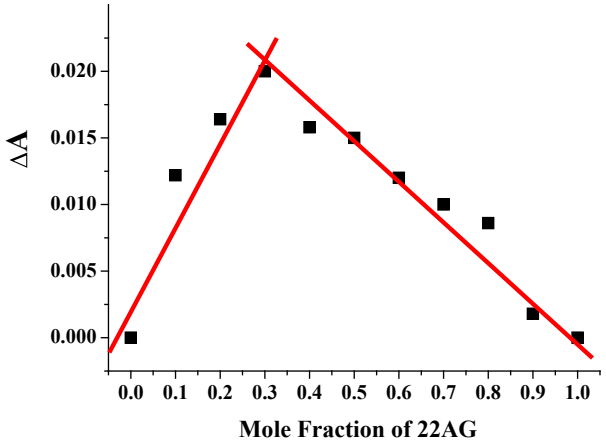

Fig. 2. Assessment of the stoichiometry of 2/DNA complex *via* Job plot analysis of UV–vis spectra.

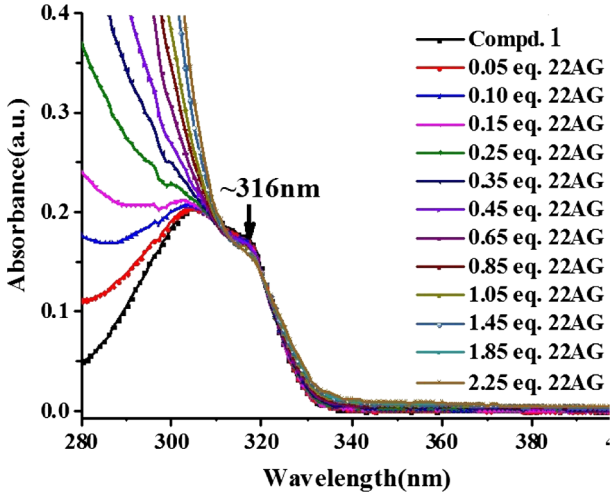

Fig. 3. UV–vis spectra of 1 (15 μM) upon addition of G4-DNA.

oligomers could be synthesized without the perturbation of cyclomers. Moreover, solely one column purification can give five products: dimer (**b**), trimer (**c**), tetramer (**d**) to pentamer (**e**) and hexamer (**f**) in the yields of 31%, 26%, 12%, 8%, 5%, respectively (Scheme 1). These compounds were fully characterized (Figs. S1–S15). Due to the difference of molecular symmetries, ^{1}HNMR patterns of even-numbered oligomers (dimer, tetramer and hexamer) are different from those of odd-numbered ones (trimer and pentamer). One of the remarkable differences is the pattern of protons of *N*-methylene. Take dimer (Fig. S1) and trimer (Fig. S4) for examples, the former's methylene protons exhibit a singlet peak (~4.97 ppm) whereas the latter ones display two peaks with the ratio of 1:2 (~5.34 and ~5.27 ppm). This typical difference makes one easy to recognize even-numbered oligomers from the odd-numbered ones.

With these TEG-derivated oligomers at hands, their solubility at physiological pH were measured, but the results were not good. Thus, these molecules were further reacted with *N*,*N*-dimethylethylenediamine to give the amino-derivated oligomers (from **2** to **6**, Scheme 1). These reactions worked smoothly in the yields of higher than 60%. Moreover, the solubilities of these amino-substituted oligomers at physiological pH were remarkably enhanced. These amino-derivated oligomers were also fully characterized (Fig. S16–S40).

3.2. Cytotoxicity

With these compounds at hands, their antiproliferative activities were assessed on four human tumor cell lines in vitro (Table 1): MCF-7

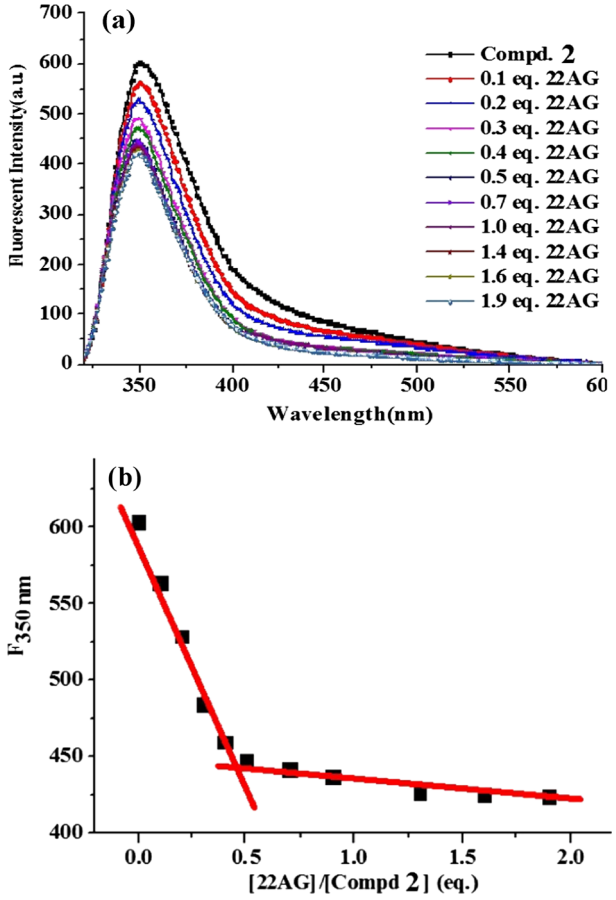

Fig. 4. (a) Fluorescence spectra of 2 (15 μM) upon addition of 22AG. (b) The plotted curve of F_{350nm} of 2 as a function of the ratio [DNA]/**[2]**.

(human breast cancer cell), HepG2 (human liver carcinoma cell), HT29 (human colon cancer cell) and A375 (human malignant melanoma cell) by using MTT assay.

Except for compound **6**, all the other compounds showed moderate activities at micromolar concentrations. In this family, the dimer compound **2** exhibited the most distinctive antitumor ability. Its IC_{50} values against HT-29, HepG2, A375 and MCF-7 were 0.69, 5.09, 3.15 and 3.8 μmol/L, respectively. Even compared with three positive-control drugs (5-fluorouracil, doxorubicin and paclitaxel), **2** was still a competitive lead compound. Moreover, the inhibitory activity of **2** towards HT-29 was better than all the other compounds tested in this study. It is really interesting to see this result because most reported carbazoles barely exhibited antiproliferative activity towards HT-29, although their inhibitory abilities against HepG2, A375 and MCF-7 were known [4–6].

It could also been observed from Table 1 that the activity of the dimer (**2**) was not only higher than that of the monomer, but also higher than those of the trimer (**3**), tetramer (**4**), pentamer (**5**) and hexamer (**6**). It indicated that the degree of polymerization should not be the reason for their different antiproliferative activities. As literature showed that some carbazole derivatives could bind to and stabilize G4-DNA, which accounted for their antiproliferative activities due to the downregulation of the expression of their target genes [4–6], we then evaluated the G4-DNA binding abilities of **2**, and used its monomeric form **1** as the control.

3.3. DNA binding study

Fig. 1a listed UV–vis spectra of **2** upon addition of G4-DNA. It could be seen that the addition of DNA caused a hypochromic and bathochromic spectra of **2** at ~305 nm. Moreover, the isosbestic point at ~330 nm could be observed, although the isosbestic point between

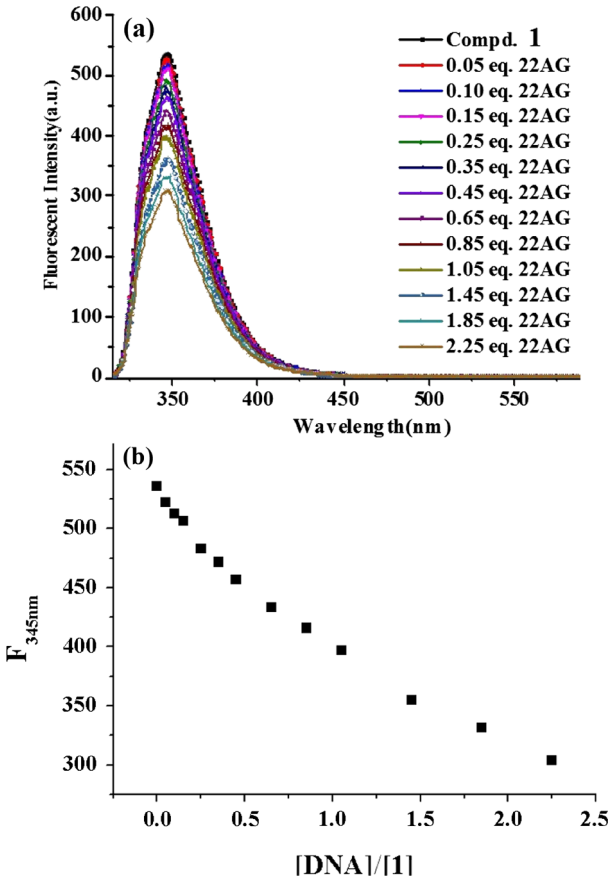

Fig. 5. (a) Fluorescence spectra of 1 (15 μM) upon addition of 22AG. (b) The plotted curve of F_{350nm} of 1 as a function of the ratio [DNA]/**[1]**.

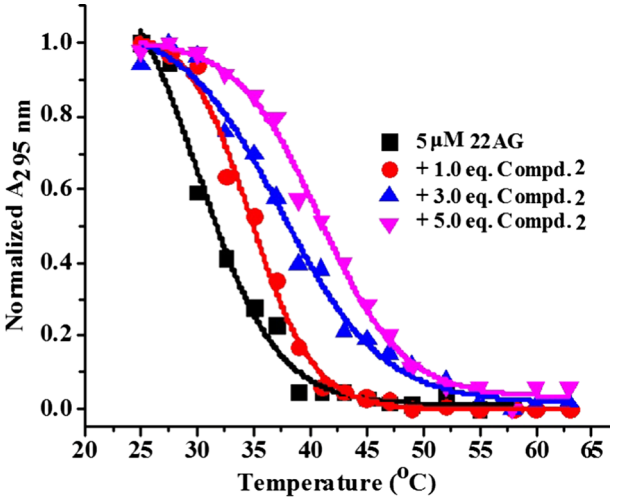

Fig. 6. UV thermal denaturation profile of G4-DNA (5 μM) before and after addition of 2.

300–310 nm was not very clear due to the disturbance of the increased absorption of G4-DNA. Based on our previous results, the above spectra pattern usually indicated that **2** specifically interacted with G4-DNA. We then plotted the curve of A_{320nm} as a function of the ratio of **[DNA]/[2]** (Fig. 1b). It could be seen that the point of inflection took place at 0.5, which indicated that two compounds were accommodated by per DNA. Job plot (Fig. 2) showed that apex point appeared at 0.33 DNA molar fraction (the ratio of **[DNA]**/**[DNA** + **2]** = 0.33), which further indicated the one molar DNA bound to two molar compounds. In view of the structural nature of G4-DNA, we then proposed that the molecule bound to the two G-quartet planes of G4-DNA due possibly to the π-π stacking interaction.

UV–vis spectra of the control compound **1** upon addition of G4-DNA were also recorded. It could be seen from Fig. 3 that a hypochromic and bathochromic spectra of **1** at ~316 nm took place. It indicated that **1** could also bind to G4-DNA by π-π stacking interaction. However, compared with significantly changed UV–vis spectra of **2**, **1**'s spectra changed much less obviously. It indicated that the binding of **1** to DNA was much weaker compared with **2**-DNA binding strength. Moreover, a more careful look at the spectra in the region of higher than 340 nm, one would see the slight light scattering spectra. It indicated that large size particles (precipitation) were produced during the titration, which was most possibly caused by electrostatic interaction between the positive charge of protonated amino group of **1** and the negative charge of phosphate anions of DNA. It thus showed that **1** did not interact with G4-DNA as specifically as **2** did.

To learn further the binding nature of **2** to DNA, its fluorescence spectra upon addition of DNA were recorded (Fig. 4). Fig. 4a showed that the addition of DNA gradually quenched the fluorescent intensity of **2** at 350 nm due to their π-π stacking interaction. The curve of F_{350nm} as a function of the ratio of **[DNA]/[2]** was plotted (Fig. 4b) and it showed that the point of inflection was also at 0.5. This finding was in agreement with the result from UV–vis titration, an indicative of the specific binding nature, which was, in brief, the two molar molecules bound to the two G-quartet planes of one molar G4-DNA.

The fluorescence spectra of the control compound **1** upon addition of DNA were also recorded (Fig. 5). The addition of DNA also quenched the fluorescence of **1**. The quench of the fluorescence may be caused by two reasons: (1) the binding of **1** to DNA; (2) the large size particles (precipitation) produced during **1**-DNA titration. The plotted curve of F_{350nm} (Fig. 5b) as a function of the ratio of **[DNA]/[1]** did not show a clear point of inflection. In other words, the quench of the fluorescence of **1** could not be saturated by the addition of large amount of DNA. It thus further indicated the weak and non specific G4-DNA binding nature of **1**.

To illustrate the binding strength of **2** to G4-DNA, UV–vis melting experiments of **2**/G4-DNA complexes were carried out by monitoring the absorption at 295 nm upon heating (Fig. 6). It could be seen from the profiles of temperature-dependent absorbance that $\triangle T_{1/2}$ of DNA in the presence of 1.0 eq., 3.0 eq. and 5.0 eq. of **2** were 3.0 °C, 6.5 °C and 9.5 °C, respectively. In other words, the more **2** was used, the higher the $\mathbf{T_m}$ of DNA was. This result unequivocally showed the binding nature of **2** to G4-DNA. As a comparation, Fig. 7 showed that the presence of the control compound **1** only slightly stabilized the $\mathbf{T_m}$ of DNA, and large amount of ligands could not remarkably enhance the $\mathbf{T_m}$ of DNA.

In order to gain more insight about G4-DNA selective binding nature, UV–vis spectra of **2** upon binding to duplex DNA were measured. Fig. 8 showed that addition of duplex DNA decreased the absorbance of **2** at 305 nm. However, the remarkable light scattering spectra could be observed in the region of higher than 340 nm. As mentioned earlier, the pattern indicated that large size particles (precipitation) were produced during the titration and it was most possibly caused by electrostatic interaction between the positive charge of protonated amino group of **2** and the negative phosphate anions of DNA. UV–vis melting experiments of **2**/duplex-DNA complexes were also carried out by monitoring the absorption at 260 nm upon heating. Fig. 9 showed that **2** barely enhanced the $\mathbf{T_m}$ of duplex DNA even if large amount of **2** was used. This finding indicated that **2** could not bind to the grooves of duplex DNA. The above results illustrated that **2** bound to duplex DNA solely by non-specific electrostatic interaction, rather than the specific groove interaction, so that it could not stabilize the $\mathbf{T_m}$ of duplex DNA. It thus indicated that **2** was a G4-DNA selective ligand.

Compound **2** was a non-rigid molecule and it was truly flexible: the symmetrical two carbazolyl units of **2** did not interact with each other because no any correlations peaks between these two parts were observed in its 2DCOSY/NOESY spectra (Fig. S19 and S20). As such, the

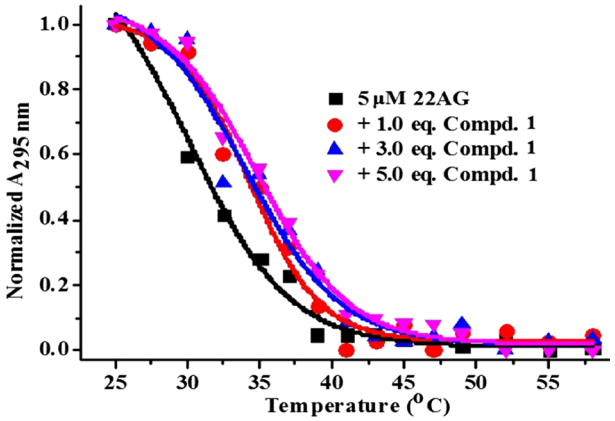

Fig. 7. UV thermal denaturation profile of G4-DNA (5 μM) before and after addition of 1.

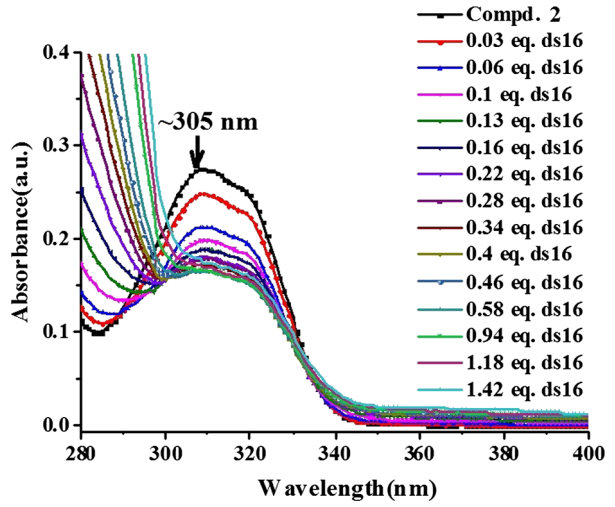

Fig. 8. UV–vis spectra of 2 (15 μM) upon addition of duplex DNA.

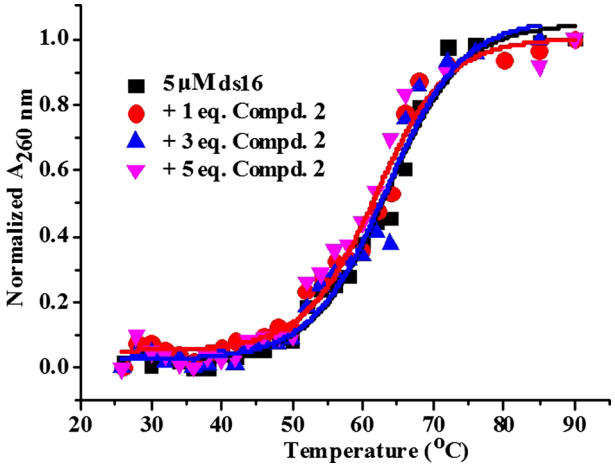

Fig. 9. UV thermal denaturation profile of duplex-DNA (5 μM) before and after addition of 2.

interaction of **2** with G4-DNA was certainly not because that it possessed a particular conformation, but rather because that the tetraquartets of G4-DNA was large enough to accommodate the relatively large methylene-bridged biscarbazole. On the other hand, the relatively large geometry of **2** prevented it from binding to the grooves or intercalating into the base pairs of duplex DNA, which thus contributed to the specificity of its interaction with G4-DNA.

4. Conclusions

In conclusion, we recently synthesized a series of conformationally flexible methylene-bridged carbazolyl oligomers and evaluated their antitumor and DNA binding activities. Among them, the dimer compound **2** exhibited the best antiproliferative activities against HT-29, HepG2, A375 as well as MCF-7 cell due possibly to its selective G4-DNA binding nature.

Acknowledgment

We thank Natural Science Foundation of Liaoning Province (20180550874), Foundation of Higher Education of Guangdong (2016KTSCX146), Natural Science Foundation of Guangdong Province (2018A0303130245).

Appendix A. Supplementary material

Supplementary data to this article can be found online at https://doi.org/10.1016/j.bioorg.2019.103074.

References

[1] S. Mondal, S. Bandyopadhyay, M.K. Ghosh, S. Mukhopadhyay, S. Roy, C. Mandal, Natural products: promising resources forcancer drug discovery, Anti-Cancer Agents Med. Chem. 12 (2012) 49–75.
[2] A.W. Schmidt, K.R. Reddy, H.-J. Knölker, Occurrence, biogenesis, and synthesis of biologically active carbazole Alkaloids, Chem. Rev. 112 (2012) 3193–3328.
[3] S. Balasubramanian, L.H. Hurley, S. Neidle, Targeting G-quadruplexes in gene promoters: a novel anticancer strategy? Nat. Rev. Drug Discovery 10 (2011) 261–275.
[4] C.C. Chang, J.Y. Wu, C.W. Chien, W.S. Wu, H. Liu, C.C. Kang, L.J. Yu, T.C. Chang, A fluorescent carbazole derivative: high sensitivity for quadruplex DNA, Anal. Chem. 75 (2003) 6177–6183.
[5] T. Das, D. Panda, P. Saha, J. Dash, Small molecule driven stabilization of promoter G-quadruplexes and transcriptional regulation of c-MYC, Bioconjug. Chem. 29 (2018) 2636–2645.
[6] B. Maji, K. Kumar, M. Kaulage, K. Muniyappa, S. Bhattacharya, Design and synthesis of new benzimidazole–carbazole conjugates for the stabilization of human telomeric DNA, telomerase inhibition, and their selective action on cancer cells, J. Med. Chem. 57 (2014) 6973–6988.
[7] S. Neidle, Quadruplex nucleic acids as targets for anticancer therapeutics, Nat. Rev. Chem. 1 (2017) 0041.
[8] G. Li, X. Zhou, P. Yang, Y. Jian, T. Deng, H. Shen, Y. Bao, Synthesis of a novel methylene-bridged biscarbazole derivative and evaluation of its DNA and nucleotide binding properties, Tetrahedron Lett. 55 (2014) 7054–7059.
[9] P. Yang, Y. Jian, X. Zhou, G. Li, T. Deng, H.Y. Shen, Z.Z. Yang, Z.M. Tian, Calix[3]carbazole: one-step synthesis and host–guest binding, J. Org. Chem. 81 (2016) 2974–2980.
[10] G. Li, X. Song, H. Yu, C. Hu, M. Liu, J. Cai, L. Zhao, Y. Chen, P. Yang, Supramolecular recognition of A-tracts DNA by calix[4]carbazole, Sensor. Actuat. B 259 (2018) 177–182.
[11] Z.Z. Yang, Y. Chen, G. Li, Z.M. Tian, L. Zhao, X. Wu, Q. Ma, M.-Z. Liu, P. Yang, Supramolecular recognition of Three Way Junction DNA by a cationic calix[3]carbazole, Chem. – Eur. J. 24 (2018) 6087–6093.
[12] P. Yang, Q. Yang, X. Qian, Novel DNA bis-intercalators of isoquinolino [4,5-bc] acridines: design, synthesis and evaluation of cytotoxic activity, Tetrahedron 61 (2005) 11895–11901.
[13] P. Yang, A. DeCian, M.-P. Teulade-Fichou, J.-L. Mergny, D. Monchaud, Engineering bisquinolinium/thiazole orange conjugates for fluorescent sensing of G-quadruplex DNA, Angew. Chem. Int. Ed. 48 (2009) 2188–2191.
[14] P. Yang, J. Singh, S. Wettig, M. Foldvari, R.E. Verrall, I. Badea, Enhanced gene expression in epithelial cells transfected with amino acid-substituted gemini nanoparticles, Eur. J. Pharm. Biopharm. 75 (2010) 311–320.
[15] S.K. Kutz, C. Börger, A.W. Schmidt, H.J. Knölker, Synthesis of methylene-bridged biscarbazole alkaloids by using an ullmann-type coupling: first total synthesis of murrastifoline-C and murrafoline-E, Chem. Eur. J. 22 (2016) 2487–2500.
[16] H. Kandemir, M.F. Saglam, I.F. Sengul, Synthesis of methylene bridged bis-pyrrolo [3,2-c]carbazoles via an unusual vilsmeier–haack product of N-ethylcarbazole polycyclic aromatic compounds. http://doi.org/10.1080/10406638.2018.1458739.